A review of chemical vapour deposition of graphene on copper†

Cecilia Mattevi,*[a] Hokwon Kim[a] and Manish Chhowalla*[ab]

Received 5th July 2010, Accepted 4th October 2010
DOI: 10.1039/c0jm02126a

The discovery of uniform deposition of high-quality single layered graphene on copper has generated significant interest. That interest has been translated into rapid progress in terms of large area deposition of thin films *via* transfer onto plastic and glass substrates. The opto-electronic properties of the graphene thin films reveal that they are of very high quality with transmittance and conductance values of >90% and 30Ω/sq, both are comparable to the current state-of-the-art indium tin oxide transparent conductor. In this Feature Article, we provide a detailed and up to date description of the literature on the subject as well as highlighting challenges that must be overcome for the utilization of graphene deposited on copper substrates by chemical vapour deposition.

Introduction

The unique properties of graphene have triggered numerous fundamental and technological studies. It is well known that graphene is a semimetal where the charge carriers behave as Dirac fermions (zero effective mass),[1] which gives rise to extraordinary effects such as mobilities up to 200000 $cm^2V^{-1}s^{-1}$,[2] ballistic transport distances of up to a micron at room temperature,[3] half-integer quantum Hall effect,[3,4] and absorption of only 2.3% of visible light.[5] The large carrier mobilities also make it potentially useful for high frequency electronic devices[6] while the low absorbance complemented with its semi-metallic nature makes it an ideal transparent conductor where transparency and low resistance are required.[7] Integrated devices will require wafer scale deposition that can be processed using existing or post complementary metal oxide semiconductor (CMOS) fabrication techniques. Implementation as a transparent conductor will require uniform deposition over large areas with controllable number of graphene layers. These requirements have led to the development of a rapidly evolving research thrust within the field of graphene based on deposition of high quality and uniform thin films over large areas with controllable thickness.

The best quality graphene, in terms of structural integrity, is obtained by mechanical cleavage of highly oriented pyrolytic graphite.[8] Thus the efficacy of any new deposition methods is determined by comparison with properties of pristine mechanically exfoliated graphene. Although pristine graphene has very low concentration of structural defects, which makes it interesting for fundamental studies, the flake thickness, size and location are largely uncontrollable. Several strategies are presently being pursued to achieve reproducible and scalable graphene on substrates. One example is covalent[9,10] or non-covalent[11] exfoliation of graphite in liquids. These methods however can introduce structural and electronic disorder in the graphene.[12–14] Another example is the conversion of SiC(0001) to graphene *via* sublimation of silicon atoms at high temperatures.[15] High quality wafer scale graphene with switching speeds of up to 100GHz[6] has been demonstrated using this technique. Although the price of the initial SiC wafer is relatively high compared to that of silicon, the technique maybe suitable for radio and THz frequency electronics where the excellent performance of the devices could offset the cost of the wafers.

The most promising, inexpensive and readily accessible approach for deposition of reasonably high quality graphene is chemical vapor deposition (CVD) onto transition metal substrates such Ni,[16] Pd,[17] Ru,[18] Ir[19] or Cu.[20] In particular, recent developments on uniform single layer deposition of graphene on copper foils over large areas have allowed access to high quality material.[20,21] Although CVD of graphene on copper is relatively new, several groups around the world have already reported excellent device characteristics such as mobilities of up to 7350 $cm^2 V^{-1}s^{-1}$ at low temperature and large area growth (up to 30 inches).[21] In this article, we provide a detailed review of the most important aspects of graphene growth on copper by CVD.

Graphene on transition metals

The formation of few layered graphene resulting from preparation of transition metal surfaces and in industrial heterogeneous catalysis[22] has been known for nearly 50 years.[22] In fact, the concept of combining carbon with other materials and then dissociating it to form graphite was first proposed in 1896.[23,24] Layers of graphite were first observed on Ni[22,25,26] surfaces that were exposed to carbon sources in the form of hydrocarbons or evaporated carbon. At about the same time, the formation of thin graphite layers on single crystal Pt[27,28] substrates was observed in catalysis experiments. It was surmised that the formation of graphite was the consequence of diffusion and segregation of carbon impurities from the bulk to the surface during the annealing and cooling stages. The interest in graphene has led to the revaluation of these methods for controllable deposition. Indeed, graphene growth has been demonstrated on a variety of transition metals [Ru,[18,29] Ir,[19,30] Co,[31] Re,[32] Ni,[33–35] Pt,[31,36] Pd[31,37]] *via* simple thermal decomposition of hydrocarbons on the surface or surface segregation of carbon upon cooling from a metastable carbon–metal solid solution. The

[a]*Materials Department, Imperial College, London, SW7 2AZ, UK. E-mail: c.mattevi@imperial.ac.uk*
[b]*Materials Science and Engineering, Rutgers University, Piscataway, NJ, 08854, USA. E-mail: manish1@rci.rutgers.edu*
† This paper is part of a *Journal of Materials Chemistry* themed issue on Chemically Modified Graphenes. Guest editor: Rod Ruoff.

carbon solubility in the metal and the growth conditions determine the deposition mechanism which ultimately also defines the morphology and thickness of the graphene films.

Graphene can grow on several hexagonal or other crystallographic surfaces. Growth on hexagonal substrates is frequently referred to as epitaxial even if significant lattice match is absent between the graphene and substrate. For lattice mismatch of less than 1%[19] as on Co(0001)[31] and Ni (111)[33] surfaces, graphene growth is commensurate with the substrate lattice. In contrast, lattice mismatch between graphene and Pt(111),[38] Pd(111),[38] Ru(111)[29] and Ir(111)[30] is >1% and therefore growth is incommensurate as indicated by the observation of Moiere patterns. The growth on Ir(111)[39,40] is particularly interesting because the Moiere patterns indicate a template on the graphene surface for sparse adsorption of hydrogen, resulting in a superlattice structure of graphane islands that induce a band gap of 0.5–0.73 eV[40] at the Fermi level. The appearance of a band gap is particularly appealing for graphene TFTs capable of exhibiting large on/off ratios.

Recent results of growth on relatively inexpensive polycrystalline Ni[16,34,35,41] and Cu[20] substrates have triggered interest in optimizing CVD conditions for large area deposition and transfer. Graphene deposited on polycrystalline Ni and transferred onto insulating substrates exhibit mobility values[16] of up to 3650 $cm^2V^{-1}s^{-1}$ and half-integer quantum Hall effect.[16] However, the fundamental limitation of utilizing Ni as the catalyst is that single and few layered graphene is obtained over few to tens of microns regions and not homogeneously over the entire substrate.[34] The lack of control over the number of layers is partially attributed to the fact that the segregation of carbon from the metal carbide upon cooling occurs rapidly within the Ni grains and heterogeneously at the grain boundaries.

In contrast to Ni, exceptional results in terms of uniform deposition of high quality single layered graphene over large areas have been recently achieved on polycrystalline copper foils.[20] The initial[20] and subsequent follow-on[21,42–50] studies have demonstrated the growth of single layered graphene over areas as large as 30-inches. Detailed imaging and spectroscopic analyses have revealed that over 95% of the copper surface is covered by single layered graphene while the remaining graphene is 2-3 layers thick, independent of growth time or heating and cooling rates.[20] The growth on copper is simple and straightforward, making high quality graphene over large area readily accessible. Furthermore, thin copper foils are inexpensive and can be easily etched with solvents available in most laboratories so that transfer onto desired substrates can be readily achieved. These features as well as the fact that copper is inexpensive, make it an appealing process for the deposition of graphene.

Graphene from silicon carbide and transfer onto insulating substrates

In addition to CVD methods, epitaxial growth of graphene is also achievable on insulating SiC(0001)[6,15] substrates *via* sublimation of silicon atoms and graphitization of remaining C atoms by annealing at high temperature (1000–1600 °C). Epitaxial graphene on SiC(0001) has been demonstrated to exhibit high mobilities, especially multilayered films. Recently single layered SiC converted graphene over a large area has been reported and shown to exhibit outstanding electrical properties.[51]

For electronic applications, graphene on insulating substrates such as plastic foils, glass or SiO_2/Si wafers is required. Presently, transfer of the as-grown graphene from metallic surfaces onto desired insulating substrates using various different methods is performed.[16,21,52] The most straightforward method for transferring graphene grown on metals is to chemically etch the metal away to obtain free floating graphene membranes that can be scooped onto desired substrates.[16] Wet etching of substrates such as Ni and Cu[53] are feasible but is challenging for metals such as Ru, Ir, Pd, Pt.[54] Dry transfer methods such as peeling of mm sized flakes of epitaxial graphene from SiC(0001) using a bilayer of Au/Polyamide[55] stamp has been demonstrated.

In the remainder of the feature article, we describe the state-of-the-art of graphene growth on copper along with recent advancements towards transfer and direct deposition onto insulating substrates. We highlight possible mechanisms for graphene growth on copper, which may be helpful in depositing the material directly onto insulating substrates. We also describe the state-of-the-art in terms of opto-electronic properties of the transferred graphene thin films and end with conclusions and outlook for graphene on copper.

Substrate requirements for graphene growth

Copper has been shown to catalyse the growth of several carbon allotropes such as graphite,[56] diamond,[57] carbon nanotubes[58,59] and most recently graphene[20] as shown in Fig. 1. The growth of graphite on copper was unintentionally achieved in 1991[56,60] in experiments designed to catalyze the growth of diamond by CVD. In these initial experiments, single and multi layered graphene were produced on (100),[56,60] (110),[56,60] (111),[56,60] and (210)[60] copper surfaces *via* carbon implantation at elevated temperatures

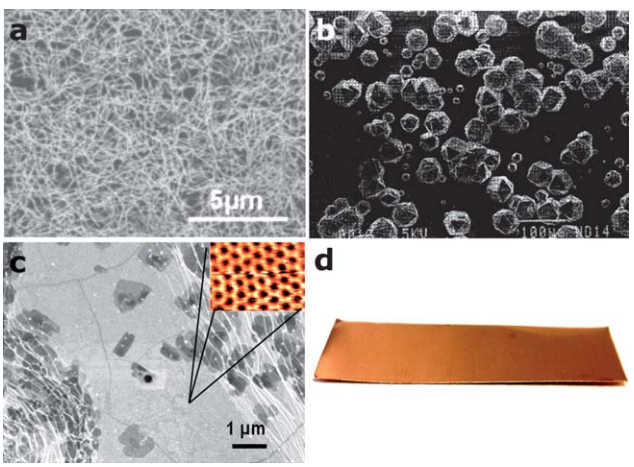

Fig. 1 SEM images of carbon allotropes grown on Cu: (a) random network of single walled carbon nanotubes.[58] Reprinted with permission from Ref. 58, copyright 2006, American Chemical Society. (b) Diamond on Cu(111).[57] Reprinted with permission from Ref. 57, copyright 1997, Elsevier. (c) Single layer graphene,[80] the inset shows STM atomic resolution images of graphene; (d) as received copper foil used as the substrate. In panel (c) dark regions represent nucleation sites. Terraces on the copper surface are also visible.

and subsequent out-diffusion through carbon dissolution-precipitation mechanism. Specifically, carbon implantation into Cu was achieved by bombarding at 70–200 keV (with doses of up to 10^{18} ions/cm^2) at 800–1000 °C. After bombardment, the implanted copper was held at 800–1000 °C for several hours to allow carbon to diffuse to the surface where it precipitated into graphitic planes. Based on the implantation study observations which was designed to grow diamond, the researchers switched to hot filament CVD (HFCVD)[57] to deposit diamond but observed thin graphite on copper substrates under some conditions.

The requirement of high quality graphite as moderators in nuclear reactors in the early 1960s[61] led to substantial knowledge of crystalline sp^2 carbon formation on hot transition metal surfaces.[25] The precipitation of graphite *via* formation of transition metal and carbon solid or liquid solution (either by exposure to hydrocarbons[25,26,36,38] or deposition of amorphous carbon on the hot metal surface[62,63]) has been widely studied and the mechanisms have been verified for all known catalysts for graphite (*i.e.* the transition metals belonging to the VIII group). Although many different experimental conditions have been found to be important, the graphite properties have been shown to be very sensitive to cooling rate and exposure time to carbon source. In addition to pure transition metals, carbides of transition metals such as TaC,[64] WC,[64] TiC,[64] HfC[64] and LaB_3[65] that have high coordination numbers and are highly reactive can also serve as catalysts for graphite precipitation.[54,66]

Of the various transition metals, graphitic carbon formation on Ni has been intensively studied owing to its suitability as catalyst for high quality graphite[25] as well as nanotubes.[67] Here we briefly describe the formation of highly crystalline sp^2 carbon on Ni to contrast it with a different formation mechanism on copper. The phase diagram of Ni and C (Ref. 68) reveals that the solubility of carbon in nickel at high temperature (above ~800 °C) forms a solid solution and lowering the temperature decreases the solubility, allowing carbon to diffuse out of Ni (Fig. 2a). It is well known from metallurgical studies that the formation of metastable Ni_3C phase promotes the precipitation of carbon out of Ni. Carbon preferentially precipitates out at the grain boundaries of polycrystalline Ni substrates so that the thickness of the graphite at the grain boundaries is substantially larger than within the grains. Thus, the number of graphene layers can significantly vary along the surface of Ni. Co and Fe show similar catalytic behaviour as can be surmised from the phase diagrams [Fig. 2b and 2c, respectively[68]], which show carbon solubility at 850–1000 °C while carbide and graphitic phases are stable at lower temperatures.[63] Like Ni, Co forms a metastable carbide at high temperature which separates into pure metal and graphite during cooling of the cobalt-carbon solid solution (Fig. 2b). In the case of Fe (Fig. 2c), cementite (Fe_3C) is a stable carbide and therefore graphite precipitation from Fe can be obtained only under very specific cooling rates.[63] The ability to form sp^2 crystalline carbon from solid solutions of various transition metals is dependent on their carbon affinity. That is, in the case of Fe there is competition between the formation of graphitic carbon and carbide owing to the high affinity between Fe and C.

The catalytic power of transition metals and some of their compounds is well known[54,66] and arises from partially filled d-orbitals or from the formation of intermediate compounds that adsorb and activate the reacting substances. Catalysis by metals results from their ability to provide low energy pathways for reactions either by facile change of oxidation states or by formation of appropriate intermediates. In light of this, Fe has asymmetrical distribution of electrons in the d-shell {[Ar]3d^{6}4s^2}, leading to mutual repulsion which may explain its higher affinity towards carbon[54] with respect to Co, Ni and Cu where the 3d shell is progressively filled, suggesting less reactive configurations (Table 1). Copper has the lowest affinity to carbon as reflected by the fact that it does not form any carbide phases[69,70] (Fig. 2d) and has very low carbon solubility compared to Co and Ni (0.001–0.008 weight % at ~1084 °C for Cu,[66,70] ~0.6 weight % for Ni at ~1326 °C, and ~0.9% weight for Co at ~1320 °C)[68] (Fig. 2). The low reactivity with carbon can be attributed to the fact that copper has a filled 3d-electron shell {[Ar]3d^{10}4s^1}, the most stable configuration (along with the half filling 3d^5) because the electron distribution is symmetrical which minimizes reciprocal repulsions. As a result, Cu can form only soft bonds with carbon *via* charge transfer from the π electrons in the sp^2 hybridized carbon to the empty 4s states of copper.[54,71] Hence this peculiar combination of very low affinity between carbon and copper along with the ability to form intermediate soft bonds makes copper a true catalyst, as defined by textbooks, for graphitic carbon formation. The 3d^7 and 3d^8 orbitals of Co and Ni are between the most unstable electronic configuration (Fe) and the most stable one (Cu). Based on this, it emerges that the most suitable catalysts for graphitic carbon formation are those transition metals that have low affinity towards carbon but that are still able to stabilize carbon on their surfaces by forming weak bonds.

An interesting example of a metal that has carbon solubility at high temperature between that of nickel and copper and does not form a carbide is ruthenium. Growth of single layer graphene over large area has been achieved on polycrystalline ruthenium thin films (50–500 nm)[72] as well as on Ru(0001) single crystals.[18] The growth on Ru is carried out by enrichment of interstitial carbon *via* exposure of the substrate to ethylene (5×10^{-7} Torr at 950 °C), followed by slow cooling in UHV to 550 °C. The carbon solubility in Ru, which is lower than Ni but higher than Cu, can be lowered by applying a gradual decrease of the temperature to obtain uniform graphene nucleation and growth. Some parallels between graphene growth on Cu and unexpected single walled carbon nanotube growth on noble metals such as Ag and Au can also be made,[73] suggesting that graphene growth on Ag and Au should be possible as recently demonstrated[74,75] for Ag.

Graphene growth on copper

Graphene on copper is in principle straightforward, involving the decomposition of methane gas over a copper substrate typically held at 1000 °C. Growth of predominantly monolayer graphene on copper foil has recently been reported using hexane[47] at 950 °C to explore the possibility of using liquids precursors that could facilitate the doping of graphene during synthesis by using nitrogen and boron containing organic solvents.[47] The specific growth parameters that have been utilized for achieving the best graphene films on Cu are summarized in Table 2. Most of the depositions have been performed on copper foils with thicknesses ranging from 25–50 μm.[20,21,46–48,76] Recently graphene deposition on e-beam[43,45] and thermally evaporated[42,44] copper thin films

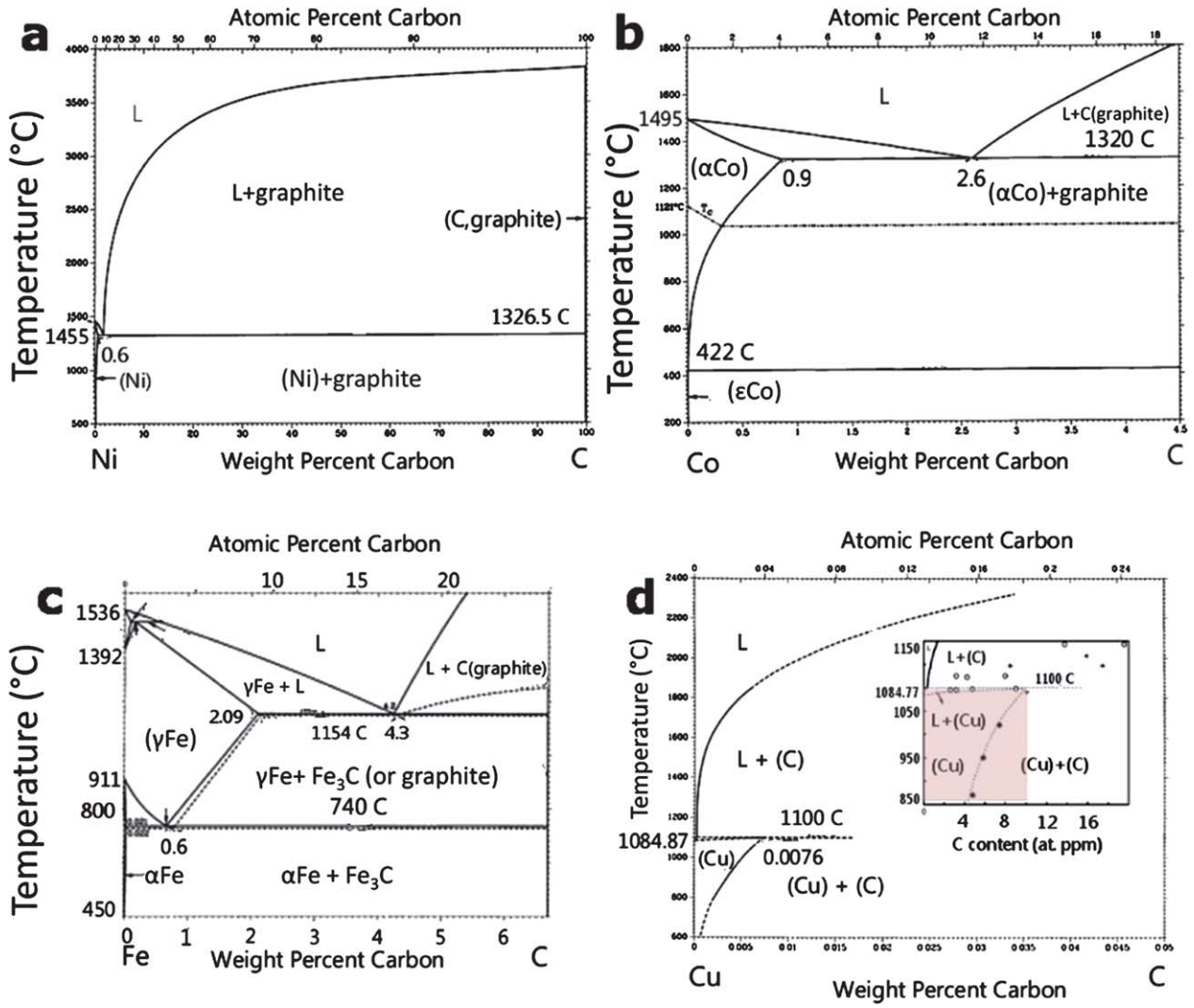

Fig. 2 Binary phase diagrams of transition metals and carbon:[68,70] (a) Ni–C; (b) Co–C; (c) Fe–C; (d) Cu–C. Reprinted with permission of ASM International®. All rights reserved, www.asminternational.org. The low carbon solubility in Cu, of ~0.008 weight % at ~1084 °C as reported in Ref. 70, is highlighted in the inset of panel (d)[70] for the temperature and composition of interest for graphene growth. Reprinted with permission from Ref. 70, copyright 2004, Elsevier.

Table 1 Carbon affinity to different transition metals is reported. The affinity decreases moving from Fe to Cu. Noble metals are indicated in the last column and listed in decreasing "noble" character from top to bottom

Fe	Co	Ni	Cu
Ru	Rh	Pt	Ag
Os	Ir	Pd	Au

(thickness > 500 nm) on SiO_2/Si substrates have been demonstrated. For thin film Cu catalysts, the thickness must be controlled to ensure that de-wetting does not occur. However, de-wetting has been used to directly deposit graphene onto insulating SiO_2/Si substrates. More specifically, recently it has been demonstrated that the copper thin films can be evaporated off after graphene growth so that the as-grown graphene rests on the insulating substrate.[43] If done controllably and reproducibly, this method could be useful for direct deposition of high quality graphene onto insulating substrates without the need for transfer. Although the most commonly used deposition temperature is 1000 °C, growth at temperatures ranging from 800–950 °C[44,50,76] have also been reported. The CVD of graphene on copper is done under low (0.5–50 Torr)[20,42] or atmospheric pressure[45] of methane and hydrogen gas mixture at various ratios as indicated in Table 2.

Copper substrate pre-treatment

Thus far, experiments have indicated that there is little influence of deposition parameters on the physical and electrical properties of as-grown graphene on copper. However, the pre-treatment of the copper foils has been found to be important in obtaining large graphene domains in the as-deposited product.[20,21] The copper substrate pre-treatment serves several important functions that ensure high quality graphene deposition. First, as-received Cu is covered by native oxide (CuO, Cu_2O),[77] which

Table 2 Summary of CVD conditions reported in the literature to grow graphene on copper

References	Growth Pressure (Torr)	Pre-annealing	H_2/CH_4 flow ratio (sccm), growth time and cooling rate	Temperature (°C)	Cu Thickness	#Graphene layers
20	0.5	1000 °C H_2 (2 sccm, 0.04 Torr) 30 min	0.06 (1min–60 min, cooling rate 40–300 °C/min)	1000	25 μm	>95% 1
42	11	(base pressure 0.1Torr) Acetic acid + heating up to 1000 °C H_2 (50–200 sccm, 2 Torr 40 °C/min)	0.23 (10–20min, cooling rate 20 °C/min + gas flow)	1000	500 nm and Cu foil 25 μm	>93% 1
76	50	900 °C 30 min H_2 10 Torr	10Torr/40Torr (10 min, cooling rate 10 °C/s) CH_4 (99.999%)	850–900	50 μm	Few layers
45	760	1. Heating up to 1000 °C in ambient pressure. 2. 30 min, 1000 °C He(1000sccm) + H_2(50sccm)	15 : 50 : 1000 sccm (H_2:CH_4:He) (5min, cooling rate in He 10 °C/s)	1000	700 nm	1,2
44	0.39	1. Ar (20sccm, 0.41Torr 12 min). 2. H_2 (20sccm,0.3Torr 1.25 min) up to 766 °C	5 (10 min) cooling in Ar 80 sccm 1Torr	800	206 nm	1,2,3
43	0.1–0.5	(pre-vacuum) Heating in H_2 up to 1000 °C	0.06 (from15 min up to 420 min) CH_4 (99.99%)	1000	100–450 nm	1
47	0.5	(pre-vacuum 0.01) Ar/H_2 400 sccm 8–9 Torr up to 950 °C	Hexane (4mL/h) 4 min	950	25 μm	1,2
80	0.3	(pre-vacuum) Heating up to 1000 °C H_2 (13 sccm, 0.1 Torr) 30 min	0.5 (30 s–30min) cooling rate 9 °C/min	1000	25 μm, 125 μm	1,2
21	1.6	Heating up to 1000 °C H_2 (8 sccm, 0.18 Torr) 30 min	0.33 (30 min) (cooling rate 10 °C/s, H_2 0.18 Torr)	1000	25 μm	1

reduces its catalytic activity. Therefore prior to deposition the Cu substrate must be annealed in a hydrogen reducing atmosphere at 1000 °C.[78] Wet chemical pre-treatment by dipping in acetic acid[79] has also been demonstrated to partially remove Cu_2O. The annealing stage prior to deposition is also important for increasing the Cu grain size and rearranging the surface morphology (introduction of atomic steps, elimination of surface structural defects) to facilitate growth of graphene flakes. Typically the Cu foils are annealed for 30 min[20,21,45,76] while shorter treatment has been reported for sub-micron Cu thin films.[42–44] A systematic correlation between the homogeneity of graphene domains and Cu grain size and crystallographic orientation has yet to be elucidated.

In Fig. 3, taken from Ref. 20, the growth of single layer graphene at different times is shown. The scanning electron microscopy (SEM) images of graphene on copper can be difficult to interpret due to the atomic thickness of the film. Here we briefly explain the evolution of the graphene film deposited on copper by describing the SEM images in Fig. 3. In Fig. 3a, graphene of finite size (one is indicated by the larger oval) in the form of dark irregularly shaped flakes can be seen. The nucleation site of one of the flakes is indicated by the smaller oval in Fig. 3a. As the growth time is increased, the graphene domains

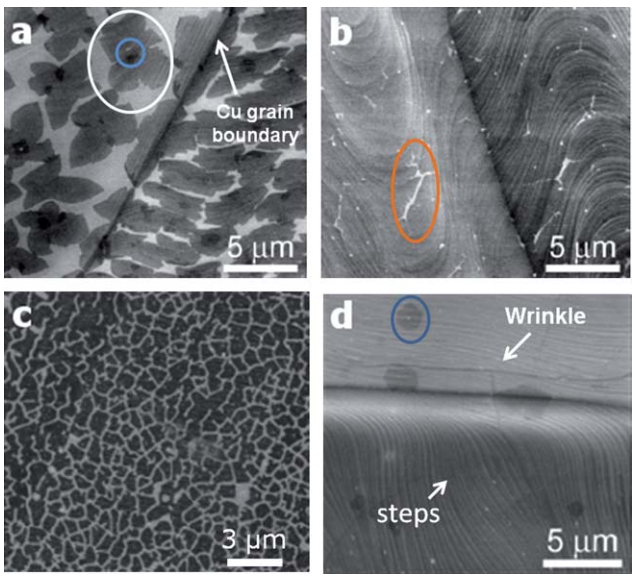

Fig. 3 SEM images of graphene on Cu for different growth times:[20] (a) 1 min; (b) 2.5 min, (c) 1 min from Ref. 80 for comparison; and (d) 10 min. In panel (a) the smaller circle represents a possible nucleation site and a Cu grain boundary is also indicated. The larger circle indicates a graphene domain. In panel (b) the highlighted region is a void where the graphene domains have yet to join to form a continuous layer. The curved lines represent terraces on the copper surface. Image in (c) is provided to highlight the differences in the nucleation density and initial domain sizes by changing the Cu pre-treatment conditions and the CH_4 pressure. The average graphene domain size is (4.8 μm ±1.2 μm) in the image shown in panel (a) while in (c) it is (0.84 ± 0.25 μm). In panel (d), SEM image of a continuous graphene film on Cu is shown. Wrinkles where the graphene domains have presumably joined along with a dark patch indicated by the circle representing a double layer are highlighted. Panel (a), (b), (d) are reprinted with permission from Ref. 20, copyright 2009, American Association for the Advancement in Science.

progressively increase in size until coalescing (Fig. 3b) into a continuous layer. Fig. 3b is an image just prior to the formation of a completely homogeneous layer, as indicated by the presence of discontinuities. One of which is indicated by the oval in Fig. 3b. The semi-continuous graphene layer is barely visible in Fig. 3b but the underlying microstructure (terraces and steps) of the Cu substrate is readily visible. It is possible to control the nucleation density and the size of the initial graphene flakes by tuning the pre-treatment conditions, the partial pressure of CH_4 and the total growth pressure as indicated by Fig. 3c. Various shapes of the nucleated graphene flakes on different Cu grains were observed,[20] perhaps suggesting that growth along a preferential Cu crystallographic directions may be favoured. After the nucleation, growth, and formation of a continuous monolayer, further exposure to the carbon precursor for up to 60 min does not lead to deposition of multilayered graphene (Fig. 3d). This is in contrast with graphene deposition on Ni where the grain boundaries introduce significant thickness inhomogeneities during growth.[34,35] It is believed that the weak interaction between graphene and the Cu substrate allows the flakes to expand over the grain boundaries with minimal structural disruption. The lateral dimensions of the Cu grain boundaries vary with the Cu foil thickness and the annealing pre-treatment time. In Fig. 3d, it can be clearly observed that the graphene grows without disruption above the Cu grain boundary, as the presence of wrinkles reveals. Our observations[80] reveal that graphene grain growth on thinner Cu foils is suppressed for identical annealing times.[80] H_2 embrittlement[77] of Cu also limits diffusion and minimizes grain growth during annealing, as indicated by the smaller initial graphene domains observed in Fig. 3c.

The as grown graphene contains wrinkles[20,56] which can be attributed to differences in the thermal expansion coefficients (TEC) between graphene or graphite with respect to copper ($\alpha_{graphene} = -6 \times 10^{-6}$/K at 27 C;[81] $\alpha_{a\text{-}graphite} = 0.9 \times 10^{-6}$/K between 600–800 °C;[82] $\alpha_{Cu} = 24 \times 10^{-6}$/K[82]). The large and negative thermal expansion coefficient of graphene (much larger than the in-plane TEC of graphite) suggests significant shrinkage of Cu upon cooling, which induces mechanical stress on graphene. This stress is released *via* the formation of wrinkles. Ridges and swells are also observed in regions where adhesion between the film and the substrate is poor. Similar phenomenon[34] has been observed for graphite grown on Ni ($\alpha = 12.89$–21.0×10^6 K^{-1} between 0–1000 °C)[83] where the wrinkling effect is more pronounced because the films are generally thicker. In addition to wrinkles, approximately 100 nm wide cracks can be also observed for graphite growth on Cu[56] (Fig. 4a).

Although there is some evidence to suggest that graphene may preferentially nucleate and grow on specific Cu crystallographic surfaces, concrete results from recent CVD studies are lacking. In previous studies with implantation,[56,60] thin graphite on several Cu crystallographic surfaces [(100),[56,60] (111),[56,60] (110),[56,60] (210)[60]] was demonstrated with c axis perpendicular to the Cu surface (Fig. 4b,c). These initial experiments yielded few layered graphene with turbostratic stacking[56] (Fig. 4b,c). Although the stacking order in CVD graphene on Cu has yet to be elucidated, Raman spectroscopy suggests that it is consisting with "turbostratic like" structure.[42,84] These results are also similar to few and multi-layered graphene grown on Ni catalysts.[35]

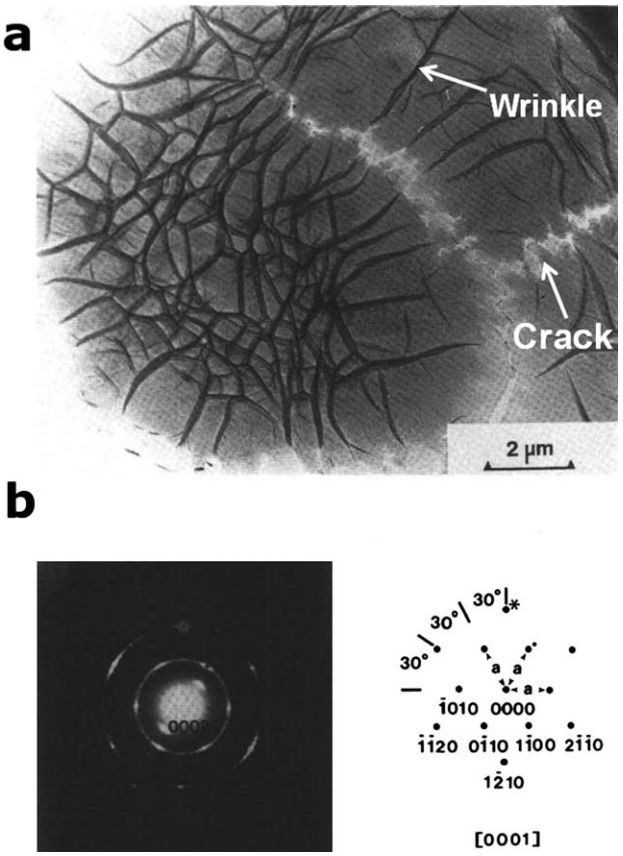

Fig. 4 (a) Transmission electron microscopy image (bright field)[56] of few layered graphene formed on Cu (111) surface after carbon implantation (70 KeV) at 820 °C. Wrinkles and cracks are readily observable. (b) The corresponding selected area electron diffraction pattern of the graphitic film along with the interpreted diffraction spots are shown. Reprinted with permission from Ref. 56, copyright, Material Research Society, Journal of Materials Research.

Surface catalysis mechanism

The growth mechanism of graphene on copper is surface related and not due to out diffusion from bulk. Substantial evidence for this has been provided by an elegant set of experiments done by the Ruoff group[84] using isotopic labelling of the methane precursor gas. By taking advantage of the fact that the Raman modes of ^{12}C and ^{13}C differ slightly in energy, they were able to monitor the progressive enlargement of graphene domains on copper. They utilized sequenced dosing of $^{12}CH_4$ and $^{13}CH_4$ (99.9% pure)[84] into the growth furnace on copper and measured the distribution of ^{12}C and ^{13}C graphene domains. In the case of solid solution and out diffusion growth mechanism (as is the case for Ni catalysts), a random mix of the isotopes in the graphene film is expected. In contrast, Raman analysis on transferred graphene on Cu reflected the dosing sequence of the two types of precursors. They found regions having close to pure ^{12}C, regions of isotopically pure ^{13}C, and regions where both ^{12}C and ^{13}C were present. The Raman bands corresponding to both ^{12}C and ^{13}C were likely from junctions between two graphene domains or from nucleation sites.

From the analysis of Raman peaks, it is possible to obtain useful structural information about graphene. The map of the

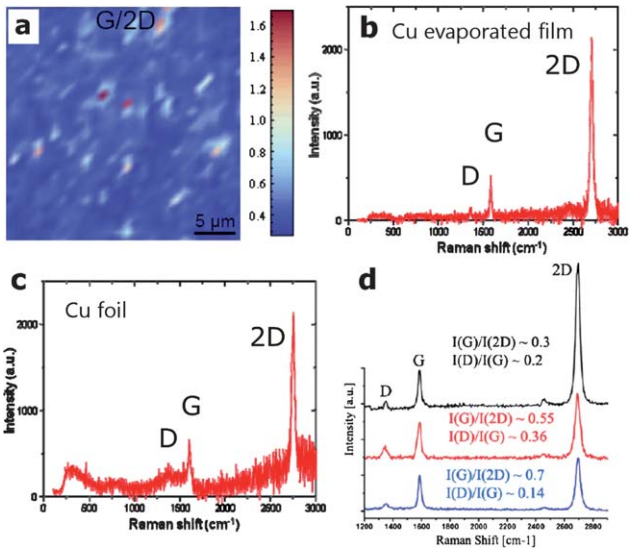

Fig. 5 (a) Raman map of a single layer graphene grown on bulk Cu substrate and transferred onto an insulating subtrate. The results indicate that over 93% of the film is monolayered[42] (2D/G = 2.5). (b) Raman spectra taken from a graphene film grown on a thin film of copper. The results suggest that the quality of graphene is comparable to that grown on foils[42] (c) (spectrum after subtraction of the background[42]). No detectable increase of D peak was observed after transfer in either case. Further, the D/G ratios for both cases were comparable. Reprinted with permission from Ref. 42, copyright 2009, American Chemical Society. (d) Raman spectra for 1-2-3- layers of graphene after transfer.[43] Reprinted with permission from Ref. 43, copyright 2010, American Chemical Society. An enhancement in the D-peak and a change in the G/2D peak ratio can be observed with transfer of additional layers.

G/2D Raman peaks ratios taken from Ref. 42 and shown in Fig. 5a clearly indicate that over 93% of the graphene grown on Cu is single layer (2D/G~2–4).[43,84,85] The Raman spectra of graphene grown on a thin film as well as on a foil of Cu are shown in Fig. 5b,c (Ref. 42). The degree of disorder in carbonaceous materials is indicated by the intensity of Raman D band, which can be seen to increase with the number of transferred graphene layers (Fig. 5d). Further evidence for uniformity of the as-grown graphene film can be obtained from the intensity maps of the G band. Typically the G-peak intensity of graphene on copper is uniform except in regions corresponding to wrinkles or graphene grain boundaries. What clearly emerges from isotopically labelled Raman analysis in Ref. 84 is that the growth time and cooling rate does not affect the graphene thickness. Furthermore the deposition of a continuous graphene layer leads to the passivation of the Cu surface so that multi-layered growth is dramatically hindered.

The presence of distinct nucleation sites, such as the one indicated by the small circle in Fig. 3a, may point to a route for obtaining the nucleation and growth of multi-layered graphene.[84] Detailed knowledge of the reconstruction of the Cu surface after the pre-growth treatment could provide insight into increasing the density of such graphene nucleation sites. For example it is well known from catalysis that atomically thin terraces with vicinal surfaces and edges of different dimensions are favourable nucleation sites[86] because of their high density of dangling bonds. Terraces are also formed on Cu at high temperature,[87] and have been observed in studies on graphene growth, suggesting that they could play an important in nucleation of graphene layers. However, the analysis of the parameters in Table 2 reveals that the deposition of predominantly monolayered graphene is favoured in most cases except where high pressure of CH_4 is utilized.

Based on the information in the literature and presented above, a qualitative model for the nucleation and growth of graphene on copper can be proposed. The three stages of the growth process are illustrated in Fig. 6 for graphene growth on Cu. Initially Cu foil with a copper oxide is depicted on the left schematic. The oxide is reduced by annealing in hydrogen atmosphere, which also leads to grain growth and annihilation of most of the surface defects that might be present. The uniform nucleation of graphene islands on the pre-treated Cu surface is depicted in the middle schematic in Fig. 6. These initial graphene domains may have different lattice orientations depending on the crystallographic orientations of the underneath Cu grains. As the growth time is increased, the initial graphene domains increase in size as indicated in the right panel. Eventually they coalesce into a continuous graphene film.

Transfer methods

The quality of as deposited graphene films can be characterized in a number of ways. From an electronics point of view, the carrier mobility along with the optical transparency and sheet conductance are used as the parameters to compare the quality of graphene films grown using various different and similar methods. Graphene grown on copper must be transferred onto insulating substrates to measure its opto-electronic properties. The transfer is typically done by depositing a protective polymeric [Polydimethylsiloxane (PDMS) or ploy(methylmethacrylate) (PMMA)] coating on top of the graphene thin film and etching the underlying copper in iron chloride [$FeCl_3$ in HCl/H_2O (1M-5M)].[45,88,89] Other Cu substrate etching recipes include HCl, HNO_3,[44,47] $Fe(NO_3)_3$[52] in H_2O (1M) and $(NH_4)_2SO_8$ (0.1M).[21] $CuCl_2$[90] can also be used and has the advantage over $FeCl_3$ in that it can regenerated from waste but the disadvantage is that it is more toxic. $FeCl_3$ is the most widely used[88,91] because it slowly and effectively[91] etches the copper without forming gaseous products or precipitates. In contrast, reactions during etching of Cu with nitric acid leads to the formation of H_2 bubbles which causes cracking in the graphene film and HNO_3 can also degrade the carbon sp^2 network. HCl releases corrosive vapor and the etching rate of copper is very slow.

The removal of the Cu substrate is performed by immersing the substrate with the graphene film into the etching bath[45,47,50,52,76] until a free-standing graphene membrane floating in the solution can be readily observed.[47,50,52] The membrane with the polymer coating is sufficiently strong to allow handling so that it can be easily placed on the desired substrate. Once transfer is completed, the polymer is removed (by dissolving with acetone for the case of PMMA). Recently successful transfer of graphene has been obtained by utilizing the roll-to-roll transfer method using a thermal release tape as the support polymer.[21] The results from Ref. 21 are summarized in Fig. 7, which shows the roll-to-roll transfer of a graphene film grown on a flexible (Fig. 7b) 30in diagonal plastic substrate (Fig. 7c). The authors demonstrate a large area touch screen with the transferred graphene and claim

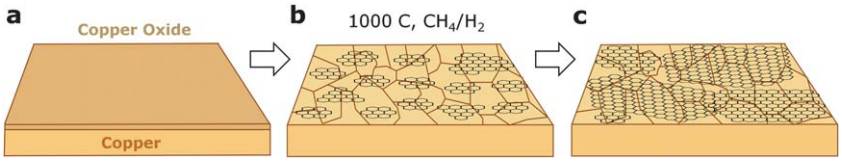

Fig. 6 Schematic illustrating the three main stages of graphene growth on copper by CVD: (a) copper foil with native oxide; (b) the exposure of the copper foil to CH_4/H_2 atmosphere at 1000 °C leading to the nucleation of graphene islands; (c) enlargement of the graphene flakes with different lattice orientations.

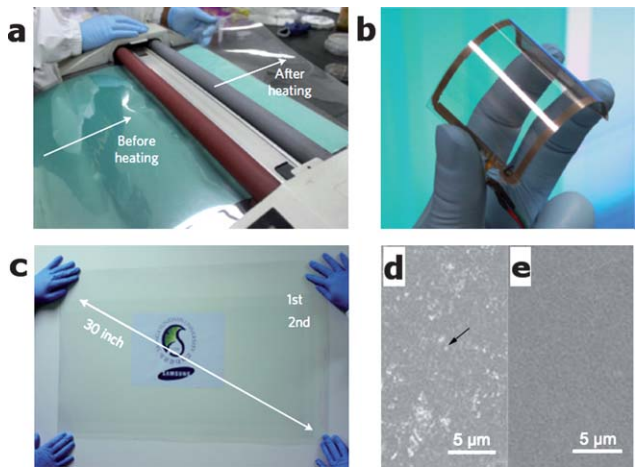

Fig. 7 (a) Roll-to-roll transfer of graphene films onto PET substrates at 120 °C using thermal release tape; (b) a flexible touch screen panel based on graphene on PET; (c) transparent graphene film transferred on a 30-inch PET sheet; (d) SEM image of single layered graphene deposited by thermal release tape. The arrow indicates defects and residual of tape; (e) SEM image of a three layers of graphene transferred by thermal release tape. Reprinted with permission from Ref. 21, copyright 2010, Nature Publishing Group. The film is free of cracks and residue from the tape.[21]

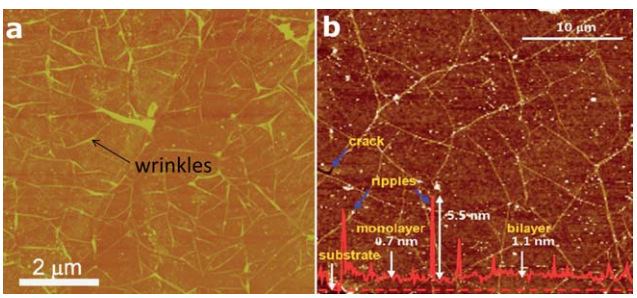

Fig. 8 Atomic force microscope images of graphene films transferred onto insulating substrates: (a) single layered graphene on SiO_2 using PMMA as the support polymer.[47] Reprinted with permission from Ref. 47, copyright 2010, American Chemical Society. (b) Single layered graphene transferred onto SiO_2 using PMMA[21] as the support polymer from a different study. Reprinted with permission from Ref. 21, copyright 2010, Nature Publishing Group.

excellent uniformity over the entire substrate. The thermal adhesive tape is proposed to be the key for transferring very large area graphene from copper to plastic substrates. Some residual thermal tape is also apparently transferred onto the substrate as indicated by the bright patches in the image in Fig. 7d of a single layer graphene. However, after three transfer cycles, a relatively clean surface free of defects is visible (Fig. 7e).

The transfer of graphene films from the copper to insulating substrates inevitably leads to cracking, as shown in Fig. 8. For graphene on Ni, cracks of up to few micro-meters have been observed[16] using PDMS as the support layer. Qualitatively, analysis of observations in the literature[21] and our own results[80] suggest that the number of cracks and defects are less when using PMMA as the support polymer in comparison to thermal release tape or PDMS. These observations are in agreement with electrical measurements which show the lowest sheet resistance on graphene films transferred with PMMA.[21,47,52] Interestingly, the electrical properties of the transferred films also depend on the substrate on which they are deposited. The lowest sheet resistance values have been obtained for graphene deposited on PET using PMMA as the support polymer (125 Ω/sq). The sheet resistance for the same graphene transferred onto a SiO_2 substrate also using PMMA as the support polymer yield values of 350 Ω/sq. This may be attributed to a higher fraction of cracking due to transfer and dissolution of PMMA when transferring on to SiO_2[52] or to interactions with charges on the oxide surface.

To minimize the cracking of transferred films, it is important to ensure good adhesion between the target substrate and the transferred graphene film. The roughness of the substrate and its hydrophobicity control the adhesion of the graphene film. Since graphene tends to maximize its contact area, a target substrate with higher roughness than the polymeric support should favour adhesion. Pre-treatments of the target substrate by hydrophobic self assembled monolayers (SAM) [perfluorophenylazide (PFPA)[92] and aminopropyl-triethoxysilane (APTES)[93]] can also enhance the adhesion of graphene by limiting crack formation during etching of the PMMA.

In principle, transfer by elastomeric stamps can avoid exposure of the graphene film to liquid etchants and the need to utilize a polymeric support. However initial attempts to carry out transfer using elastomeric stamps (PDMS) have not revealed remarkable improvements in the graphene quality. Similar results have been found for graphene grown on nickel.[16] Methods such as thermal tape and Au/polyamide have also been employed to remove graphene from bulk graphite [highly oriented pyrolytic graphite (HOPG)][94] and SiC(0001)[55] but the film uniformity was found to be compromised.

To overcome the limitations of substrate etching and transfer using elastomeric stamps, other transfer free batch fabrication methods for graphene devices have been demonstrated. In a recent study,[42] Cu catalyst in the form of thin film was deposited on $Ni/SiO_2/Si$ wafers on which graphene film was grown. Subsequent to growth, the wafer was patterned using

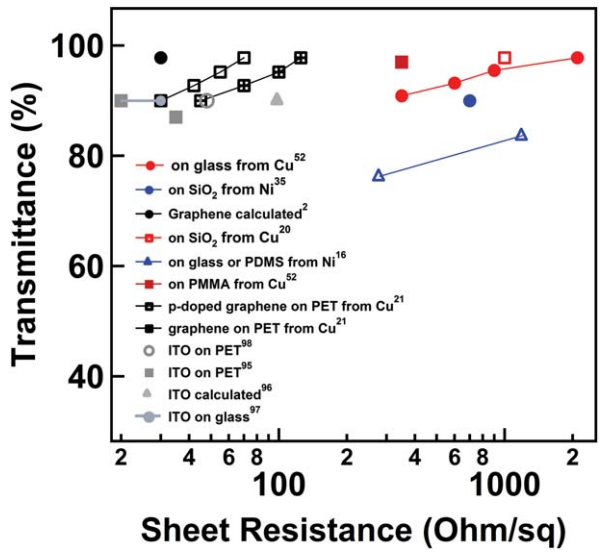

Fig. 9 Transmittance at 550 nm and the corresponding sheet resistance of graphene synthesized by CVD on Cu[20,47,50,76] and on Ni[16,35] in comparison with ITO[95–98] and calculated values of graphene[2].

photoresist after which the entire sample was etched in solution to remove Cu from unprotected regions beneath the photoresist/graphene strips, resulting in two pads of graphene/Cu connected by a narrow channel of graphene. To finish, the photoresist is removed, leaving the graphene channel resting on the substrate connected to the two contact pads.

Opto-electronic properties of graphene transferred from Cu

The exposure to various chemicals during transfer is a cause for concern in terms of introducing defects or undesirable impurities in the transferred graphene. Although a detailed study of the chemical and physical structure of transferred graphene is yet to be reported, the initial reports indicate that the high quality of graphene is apparently reasonably well preserved after transfer onto insulating substrates. Structurally, the Raman D-band does not show any remarkable increase in intensity[42] after transfer. Electronically, the highest field effect mobility for transferred films has been reported to be 4050 $cm^2V^{-1}s^{-1}$ ($n_0 = 3.2 \times 10^{11}$ cm^{-120}) but in most cases values range from 700–3000 $cm^2V^{-1}s^{-1}$[42,45,46,48] at room temperature. Recently, high carrier concentrations of $\sim 4.26 \times 10^{12}$ cm^{-1} [Ref. 21] have been reported for undoped transferred graphene films. Doping has been shown to further increase the carrier concentration up to $\sim 9.43 \times 10^{12}$ cm^{-1}.[21] It is worth pointing out that any transfer method utilizing wet etching is likely to lead to doped graphene due to the strongly oxidizing nature of the chemicals. This is corroborated by the fact that the Dirac points in the transfer characteristics of the field effect transistors are found to be situated between $V_g = 20$–60 V[21,46,48] in ambient conditions as well as in vacuum (1×10^{-5} Torr),[47] The best opto-electronic properties of the transferred films have been obtained by Bae *et al.* with Hall mobility of up to 7350 $cm^2V^{-1}s^{-1}$[21] at low temperature and 5100 $cm^2V^{-1}s^{-1}$ at room temperature,[21] and sheet resistance of 30 Ω/sq at transmittance of 90%.[21] The latter values are better than or comparable to existing state-of-the-art indium tin oxide (ITO) transparent conductors. The transparency at 550 nm and sheet resistance of graphene films produced by various methods and ITO (Ref. 95–98) are summarized in Fig. 9. The sheet resistance of graphene transferred on PET (125 Ω/sq 97.8% and 30 Ω/sq 90%)[21] are close to the theoretical values of graphene.[2] However, graphene deposited on glass yield sheet resistance values of 2100 Ω/sq.[52] The graphene grown on Cu and transferred onto glass substrate has higher transmittance with comparable sheet resistance to graphene grown on Ni.[16,35] This is most likely due to defects (grain boundaries, wrinkles) on the Ni deposited films.

Conclusions and outlook

Chemical vapor deposition (CVD) of graphene utilizing copper as the catalyst is one of the most promising methods for producing continuous layers of high quality graphene over large areas. The mechanism is surface related due to the peculiar interactions between Cu and C and therefore self-limited to a single layer of graphite. In particular, the combination of very low carbon solubility in Cu, common to noble metals that have closed d shells and strong free-electron-like surface states, along with its catalytic activity towards hydrocarbon gasses render Cu a unique catalyst. Wrinkles and grain boundaries are sparse in graphene grown on Cu and therefore excellent opto-electronic properties can be achieved. Scalable synthesis will require a better understanding and optimization of the growth process. In addition, direct deposition of graphene with controllable number of layers will be a key breakthrough. The present method of doing multiple depositions and transfers is unlikely to be viable in the long term for technological implementation, especially in large area electronics. Direct synthesis of multilayers will likely have superior electrical properties due to smaller interlayer distance and possible AB stacking. Presently, a challenging issue for graphene growth on Cu (or any other metallic substrate) is the development of a reliable and scalable transfer method. However, the real key will be to implement the knowledge obtained from the growth mechanism of graphene on Cu for direct deposition onto insulating substrates. If these challenges can be overcome then graphene grown on Cu has the potential for replacing ITO as the ubiquitous transparent conductor.

Acknowledgements

The authors thank Dr. R. Calvo and Prof. C. Hirjibehedin for providing the graphene STM image. MC acknowledges funding from the US NSF CAREER Award (ECS 0543867). CM, HK, and MC acknowledge financial support from Center for Advanced Structural Ceramics (CASC) at Imperial College London, Leverhulme Charitable Trust Grant, and the Department of Materials. M.C. acknowledges support from the Royal Society through the Wolfson Merit Award.

Bibliography

1 A. H. C. Neto, F. Guinea, N. M. R. Peres, K. S. Novoselov and A. K. Geim, *Rev. Mod. Phys.*, 2009, **81**, 109.
2 J.-H. Chen, C. Jang, S. Xiao, M. Ishigami and M. S. Fuhrer, *Nat. Nanotechnol.*, 2008, **3**, 206.

3 X. Du, I. Skachko, A. Barker and E. Y. Andrei, *Nat. Nanotechnol.*, 2008, **3**, 491.
4 X. Du, I. Skachko, F. Duerr, A. Luican and E. Y. Andrei, *Nature*, 2009, **462**, 192.
5 R. R. Nair, P. Blake, A. N. Grigorenko, K. Novoselov, T. J. Booth, T. Stauber, N. M. R. Peres and A. K. Geim, *Science*, 2008, **320**, 1308.
6 Y.-M. Lin, C. Dimitrakopoulos, K. A. Jenkins, D. B. Farmer, H.-Y. Chiu and A. Grill, *Science*, 2010, **327**, 662.
7 J. K. Wassei and R. B. Kaner, *Mater. Today*, 2010, **13**, 52.
8 K. S. Novoselov, A. K. Geim, S. V. Morozov, D. Jiang, Y. Zhang, S. V. Dubonos, I. V. Grigorieva and A. A. Firsov, *Science*, 2004, **306**, 666.
9 S. Stankovich, D. A. Dikin, G. H. B. Dommett, K. M. Kohlhaas, E. J. Zimney, E. A. Stach, R. D. Piner, S. T. Nguyen and R. S. Ruoff, *Nature*, 2006, **442**, 282.
10 G. Eda, G. Fanchini and M. Chhowalla, *Nat. Nanotechnol.*, 2008, **3**, 270.
11 Y. Hernandez, M. Lotya, D. Rickard, S. D. Bergin and J. N. Coleman, *Langmuir*, 2010, **26**, 3208.
12 C. Mattevi, G. Eda, S. Agnoli, S. Miller, K. A. Mkhoyan, O. Celik, D. Mastrogiovanni, G. Granozzi, E. Garfunkel and M. Chhowalla, *Adv. Funct. Mater.*, 2009, **19**, 2577.
13 S. De, P. J. King, M. Lotya, A. O'Neill, E. M. Doherty, Y. Hernandez, G. S. Duesberg and J. N. Coleman, *Small*, 2010, **6**, 458.
14 G. Eda and M. Chhowalla, *Adv. Mater.*, 2010, **22**, 2392.
15 W. A. de Heer, C. Berger, X. Wu, P. N. First, E. H. Conrad, X. Li, T. Li, M. Sprinkle, J. Hass, M. L. Sadowski, M. Potemski and G. Martinez, *Solid State Commun.*, 2007, **143**, 92.
16 K. S. Kim, Y. Zhao, H. Jang, S. Y. Lee, J. M. Kim, K. S. Kim, J.-H. Ahn, P. Kim, J.-Y. Choi and B. H. Hong, *Nature*, 2009, **457**, 706.
17 S.-Y. Kwon, C. V. Ciobanu, V. Petrova, V. B. Shenoy, J. Bareño, V. Gambin, I. Petrov and S. Kodambaka, *Nano Lett.*, 2009, **9**, 3985.
18 P. W. Sutter, J.-I. Flege and E. A. Sutter, *Nat. Mater.*, 2008, **7**, 406.
19 J. Coraux, A. T. N'Diaye, C. Busse and T. Michely, *Nano Lett.*, 2008, **8**, 565.
20 X. Li, W. Cai, J. An, S. Kim, J. Nah, D. Yang, R. Piner, A. Velamakanni, I. Jung, E. Tutuc, S. K. Banerjee, L. Colombo and R. S. Ruoff, *Science*, 2009, **324**, 1312.
21 S. Bae, H. Kim, Y. Lee, X. Xu, J.-S. Park, Y. Zheng, J. Balakrishnan, T. Lei, H. Ri Kim, Y. I. Song, Y.-J. Kim, K. S. Kim, B. Ozyilmaz, J.-H. Ahn, B. H. Hong and S. Iijima, *Nat. Nanotechnol.*, 2010, **5**, 574.
22 B. C. Banerjee, T. J. Hirt and P. L. Walker, *Nature*, 1961, **192**, 450.
23 E. G. Acheson. United States Patent, Sept. 29, 1896; Vol. 568323.
24 W. C. Arsem, *Ind. Eng. Chem.*, 1911, **3**, 799.
25 A. E. Karu and M. J. Beer, *J. Appl. Phys.*, 1966, **37**, 2179.
26 S. D. Robertson, *Nature*, 1969, **221**, 1044.
27 A. E. Morgan and G. A. Samorjai, *Surf. Sci.*, 1968, **12**, 405.
28 S. Hagstrom, H. B. Lyon and G. A. Somorjai, *Phys. Rev. Lett.*, 1965, **15**, 491.
29 F. J. Himpsel, K. Christmann, P. Heimann, D. E. Eastman and P. J. Feibelman, *Surf. Sci.*, 1982, **115**, L159.
30 A. Kholin, E. V. Rut'kov and A. Y. Tontegode, *Sov. Phys.–Solid State*, 1985, **27**, 155.
31 J. C. Hamilton and J. M. Blakely, *Surf. Sci.*, 1980, **91**, 199.
32 N. R. Gall, S. N. Mikhallov, E. V. Rut'kov and A. Y. Tontegode, *Sov. Phys.-Solid State*, 1985, **27**.
33 M. Eizenberg and J. M. Blakely, *Surf. Sci.*, 1979, **82**, 228.
34 A. N. Obraztsov, E. A. Obraztsova, A. V. Tyurnina and A. A. Zolotukhin, *Carbon*, 2007, **45**, 2017.
35 A. Reina, X. Jia, J. Ho, D. Nezich, H. Son, V. Bulovic, M. S. Dresselhaus and J. Kong, *Nano Lett.*, 2009, **9**, 30.
36 Z. P. Hu, D. F. Ogletree and M. A. Somorjai, *Surf. Sci*, 1987, **180**.
37 T. A. Land, T. Michely, R. J. Behm, J. C. Hemminger and G. Comsa, *Surf. Sci.*, 1992, **264**, 261.
38 J. C. Hamilton and J. M. Blakely, *Surf. Sci.*, 1980, **91**, 199.
39 J. Coraux, A. T. N'Diaye, C. Busse and T. Michely, *Nano Lett.*, 2008, **8**, 565.
40 R. Balog, B. Jorgensen, L. Nilsson, M. Andersen, E. Rienks, M. Bianchi, M. Fanetti, E. Laegsgaard, A. Baraldi, S. Lizzit, Z. Sljivancanin, F. Besenbacher, B. Hammer, T. G. Pedersen, P. Hofmann and L. Hornekaer, *Nat. Mater.*, 2010, **9**, 315.
41 Q. Yu, J. Lian, S. Siriponglert, H. Li, Y. P. Chen and S.-S. Pei, *Appl. Phys. Lett.*, 2008, **93**, 113103.
42 M. P. Levendorf, C. S. Ruiz-Vargas, S. Garg and J. Park, *Nano Lett.*, 2009, **9**, 4479.
43 A. Ismach, C. Druzgalski, S. Penwell, A. Schwartzberg, M. Zheng, A. Javey, J. Bokor and Y. Zhang, *Nano Lett.*, 2010, **10**, 1542.
44 Y.-H. Lee and J.-H. Lee, *Appl. Phys. Lett.*, 2010, **96**, 083101.
45 Y. Lee, S. Bae, H. Jang, S. Jang, S.-E. Zhu, S. H. Sim, Y. I. Song, B. H. Hong and J.-H. Ahn, *Nano Lett.*, 2010, **10**, 490.
46 D. Wei, Y. Liu, Y. Wang, H. Zhang, L. Huang and G. Yu, *Nano Lett.*, 2009, **9**, 1752.
47 A. Srivastava, C. Galande, L. Ci, L. Song, C. Rai, D. Jariwala, K. F. Kelly and P. M. Ajayan, *Chem. Mater.*, 2010, **22**, 3457.
48 H. Cao, Q. Yu, L. A. Jauregui, J. Tian, W. Wu, Z. Liu, R. Jalilian, D. K. Benjamin, Z. Jiang, J. Bao, S. S. Pei and Y. P. Chen, *Appl. Phys. Lett.*, 2010, **96**, 122106.
49 V. P. Verma, S. Das, I. Lahiri and W. Choi, *Appl. Phys. Lett.*, 2010, **96**, 203108.
50 X. S. Li; W. W. Cai; I. H. Jung; J. H. An; D. X. Yang; A. Velamakanni; R. Piner; L. Colombo; R. S. Ruoff. In *Graphene and Emerging Materials for Post-Cmos Applications*; Obeng, Y., DeGendt, S., Srinivasan, P., Misra, D., Iwai, H., Karim, Z., Hess, D. W., Grebel, H., ed; Electrochemical Society Inc: Pennington, 2009; Vol. 19, p 41.
51 X. Wu, Y. Hu, M. Ruan, N. K. Madiomanana, J. Hankinson, M. Sprinkle, C. Berger and W. A. DeHeer, *Appl. Phys. Lett.*, 2009, **95**, 223108.
52 X. Li, Y. Zhu, W. Cai, M. Borysiak, B. Han, D. Chen, R. D. Piner, L. Colombo and R. S. Ruoff, *Nano Lett.*, 2009, **9**, 4359.
53 J. McCleverty. *Chemistry of the first-row Transition Metals*; Oxford science publications, 1999.
54 A. Earnshaw; T. J. Harrington. *The chemistry of the transition elements*; Oxford University Press, 1972.
55 S. Unarunotai, Y. Murata, C. E. Chialvo, H.-s. Kim, S. MacLaren, N. Mason, I. Petrov and J. A. Rogers, *Appl. Phys. Lett.*, 2009, **95**, 202101.
56 T. P. Ong, F. Xiong, R. P. H. Chang and C. W. J. White, *J. Mater. Res.*, 1992, **7**, 2429.
57 L. Constant, C. Speisser and F. L. Normand, *Surf. Sci.*, 1997, **387**, 28.
58 W. Zhou, Z. Han, J. Wang, Y. Zhang, Z. Jin, X. Sun, Y. Zhang, C. Yan and Y. Li, *Nano Lett.*, 2006, **6**, 2987.
59 L. Ding, A. Tselev, J. Wang, D. Yuan, H. Chu, T. P. McNicholas, Y. Li and J. Liu, *Nano Lett.*, 2009, **9**, 800.
60 S.-T. Lee, S. Chen, G. Braunstein, X. Feng, I. Bello and W. M. Lau, *Appl. Phys. Lett.*, 1991, **59**, 785.
61 C. Baraniecki, P. H. Pinchbeck and F. B. Pickering, *Carbon*, 1969, **7**, 213.
62 B. C. Banerjee and P. L. Walker J., *J. Appl. Phys.*, 1962, **33**, 229.
63 F. J. Derbyshire, A. E. B. Presland and D. L. Trimm, *Carbon*, 1975, **13**, 111.
64 T. Aizawa, R. Souda, S. Otani, Y. Ishizawa and C. Oshima, *Phys. Rev. Lett.*, 1990, **64**, 768.
65 C. Oshima, E. Bannai, a. Tanaka and S. Kawai, *Jpn. J. Appl. Phys.*, 1977, **16**, 965.
66 C. Oshima and A. Nagashima, *J. Phys.: Condens. Matter*, 1997, **9**, 1.
67 S. Helveg, C. Lopez-Cartes, J. Sehested, P. L. Hansen, B. S. Clausen, J. R. Rostrup-Nielsen, F. Abild-Pedersen and J. K. Norskov, *Nature*, 2004, **427**, 426.
68 In *ASM Handbook*; ASM International: 2002; Vol. 3, Alloy Phase Diagrams.
69 R. McLellan, *Scr. Metall.*, 1969, **3**, 389.
70 G. A. Lopez and E. J. Mittemeijer, *Scr. Mater.*, 2004, **51**, 1.
71 P. Sutter, M. S. Hybertsen, J. T. Sadowski and E. Sutter, *Nano Lett.*, 2009, **9**, 2654.
72 E. Sutter, P. Albrecht and P. Sutter, *Appl. Phys. Lett.*, 2009, **95**, 133109.
73 D. Takagi, Y. Homma, H. Hibino, S. Suzuki and Y. Kobayashi, *Nano Lett.*, 2006, **6**, 2642.
74 C. A. Di, D. Wei, G. Yu, Y. Liu, Y. Guo and D. Zhu, *Adv. Mater.*, 2008, **20**, 3289.
75 J. H. Byeon and J.-W. Kim, *Appl. Phys. Lett.*, 2010, **96**, 153102.
76 W. Cai, Y. Zhu, X. Li, R. D. Piner and R. S. Ruoff, *Appl. Phys. Lett.*, 2009, **95**, 123115.
77 M. Z. Butt, *J. Mater. Sci. Lett.*, 1983, **2**, 1.
78 Y. N. Z. Trehan, *Z. Anorg. Allg. Chem.*, 1962, **318**, 107.
79 K. L. Chavez and D. W. J. Hess, *J. Electrochem. Soc.*, 2001, **148**, G640.
80 H. Kim *et al.*, in preparation, 2010.
81 W. Bao, F. Miao, Z. Chen, H. Zhang, W. Jang, C. Dames and C. N. Lau, *Nat. Nanotechnol.*, 2009, **4**, 562.

82 J. B. Nelson and D. P. Riley, *Proc. Phys. Soc.*, 1945, **57**, 477.
83 T. G. Kollie, *Phys. Rev. B: Solid State*, 1977, **16**, 4872.
84 X. Li, W. Cai, L. Colombo and R. S. Ruoff, *Nano Lett.*, 2009, **9**, 4268.
85 A. C. Ferrari, J. C. Meyer, V. Scardaci, C. Casiraghi, M. Lazzeri, F. Mauri, S. Piscanec, D. Jiang, K. S. Novoselov, S. Roth and A. K. Geim, *Phys. Rev. Lett.*, 2006, **97**, 187401.
86 H. Chen, W. Zhu and Z. Zhang, *Phys. Rev. Lett.*, 2010, **104**, 186101.
87 W. M. Robertson, *Acta Metall.*, 1964, **12**, 241.
88 E. B. Saubestre, *Ind. Eng. Chem.*, 1959, **51**, 288.
89 W. Regan, N. Alem, B. Aleman, B. Geng, C. Girit, L. Maserati, F. Wang, M. Crommie and A. Zettl, *Appl. Phys. Lett.*, 2010, **96**, 113102.
90 In *ASM Handbook Vol. 5 Surface Engineering*, 1994.
91 S. Habu and Y. Yoshihiro, *Ind. Eng. Chem. Process Des. Dev.*, 1982, **21**, 511.
92 L.-H. Liu and M. Yan, *Nano Lett.*, 2009, **9**, 3375.
93 H. A. Becerril, J. Mao, Z. Liu, R. M. Stoltenberg, Z. Bao and Y. Chen, *ACS Nano*, 2008, **2**, 463.
94 L. Song, L. Ci, W. Gao and P. M. Ajayan, *ACS Nano*, 2009, **3**, 1353.
95 H. Kim, J. S. Horwitz, G. P. Kushto, Z. H. Kafafi and D. B. Chrisey, *Appl. Phys. Lett.*, 2001, **79**, 284.
96 J.-Y. Lee, S. T. Connor, Y. Cui and P. Peumans, *Nano Lett.*, 2008, **8**, 689.
97 R. G. Gordon, *MRS Bulletin*, 2000, August, 52.
98 F. L. Wong, M. K. Fung, S. W. Tong, C. S. Lee and S. T. Lee, *Thin Solid Films*, 2004, **466**, 225.

